Catalysis Letters Vol. 103, Nos. 3–4, October 2005 (© 2005)
DOI: 10.1007/s10562-005-7157-3

Indications for metal-support interactions: The case of CO_2 adsorption on Cu/ZnO(0001)

J. Wang, S. Funk, and U. Burghaus*

Department of Chemistry, Biochemistry, and Molecular Biology, North Dakota State University, Fargo, North Dakota, USA

Received 11 March 2005; accepted 7 June 2005

Molecular beam scattering has been combined with TDS to provide consistent evidence for metal-support interactions (MSI). CO_2 adsorbs on the Cu cluster and populated the perimeter of the clusters. The Cu-free areas of the support remain essentially clean. Hence, a synergistic effect such as MSI is present.

KEY WORDS: Metal Support Interaction; adsorption dynamics; adsorption probabilities; adsorption kinetics; metal oxide surfaces; Zn–ZnO; ZnO(0001); CO_2; copper clusters; molecular beam scattering; Thermal Desorption Spectroscopy.

1. Introduction

Although we present strictly a surface science study, the results obtained and the selection of the system are interesting for applications such as heterogeneous catalysis. For example, zinc oxide is one component of the technical methanol synthesis catalyst, with CO_2 as the main source for carbon in CH_3OH (see e.g. [1, 2]). The nature of the active site remains still under controversy; $Cu^{\pm\delta}$ ions, [3] metallic copper, [4, 5] alloy formation, [2, 6–11] and defects [12] have been considered as possible candidates. In particular, the interaction of the Cu-metal deposits with the ZnO-support, and whether or not they chemically modify the support, are still rather unexplored. Molecular beam scattering techniques, as applied in the present study, could help gain a deeper understanding of possible synergistic effects such as a metal support interaction (MSI) [13–17].

Fortunately, the growths morphology of Cu on the Zn-terminated ZnO(0001) surface has thoroughly been studied by literally all surface science techniques, including electron spectroscopy [18], surface vibration spectroscopy [19], kinetic, and imaging techniques [20] as well as by theoretical [21, 22] studies. Although a dispute is still active with regard to details of the growth morphology, mostly agreement has been reached [22, 23] about the growth mode at the small and large Cu coverage, Θ_{Cu}. Accordingly, two-dimensional islands with diameters of 5–10 Å dominate the growth at very low Θ_{Cu}, and three-dimensional Cu clusters form at large Θ_{Cu} Therefore, we focus on the effect of very small and large coverages of Cu on the adsorption dynamics of CO_2.

A related molecular beam-scattering study about CO/Cu–ZnO(0001) has been presented elsewhere (see [24]). Briefly, due to the large difference in the binding energy of CO on copper and the ZnO support, the adsorption dynamics of CO was dominated by the Cu deposits. Astonishingly, a direct adsorption mechanism of the Langmuirian type, with the adsorption probability, S, of CO decreasing with coverage, Θ, i.e., $S \sim 1 - \Theta$, has been observed.

Thermal desorption spectroscopy (TDS) curves of CO_2 adsorbed on the clean support, ZnO(0001), consist of two structures which could be identified as adsorption on pristine and intrinsic defect sites with binding energies of 34.4 kJ/mol and 43.6 kJ/mol (see [25]), respectively. For Cu(110), binding energies of ~25 kJ/mol have been obtained for CO_2 (see [26]); reference data for other crystallographic orientations are not available. In contrast to CO, the binding energies of CO_2 on the copper deposits and the support are unfortunately too similar to allow sampling solely the effect of the Cu deposits. Therefore, a superposition of effects arising from the support, the deposits, and synergistic effects (metal support interactions) needs to be considered simultaneously.

In the presented study, the reactivity of the Cu-on-ZnO(0001) system towards adsorption of CO_2 at small and large Cu coverage has been characterized by adsorption probability and a set of TDS measurements. We propose that the CO_2 molecules adsorb on the Cu clusters and populate the rim of the Cu cluster leaving the ZnO support mostly clean. Therefore, a metal support interaction is present.

2. Experimental procedures

The measurements have been conducted by a home-built, triply differentially pumped molecular beam system (see [27] for details). The supersonic beam is

* To whom correspondence should be addressed.
E-mail: Uwe.Burghaus@ndsu.edu

attached to a scattering chamber which currently contains two mass filters (Stanford Research RGA100 and Pfeiffer QME200) – one of them equipped with an aperture for TDS, a Low Energy Electron Diffraction/Auger Electron Spectroscopy system (LEED/AES), a sputter gun, and a home-built metal evaporator. Copper has been vapor deposited on the surface at a temperature, T_s, of 300 K; the annealed temperature thereby never exceeding 350 K. The equivalent Cu coverage has been estimated from AES and CO-TDS measurements (see [24]). The impact energy, E_i, of the CO_2 molecules could be varied within 0.12–0.9 eV by seeding 3% CO_2 in He, combined with a variation of the nozzle temperature within 300–750 K (see [27]). It is important to note that the TDS measurements are experimentally critical in regard to contributions from the sample holder, etc. Therefore, a number of precautions have been taken. First, the mass filter used for TDS is equipped with an 8 mm (O.D.) aperture and the sample (10×10 mm crystal) to detector distance amounts to only ~2 mm. Second, the sample holder consists of a 4-pin ceramics feed-through with the air side connected to a stainless steel rod which acts as the reservoir for lN_2 (cf., e.g. [28, 29]). Thus, no bulky parts have been used in designing the sample holder, and the metal pins on which the sample is mounted stick directly into the lN_2 reservoir. This allows for good cooling performance (~ 80 K, see [25]) and eliminates the risk of contributions from the sample holder to the TDS signal. Finally, CO_2 has been dosed on the sample with the molecular beam system, which keeps the CO_2 background pressure while dosing the gas below 5×10^{-8} mbar. The reading of the thermocouple has been calibrated *in situ* by TDS measurements of *n*-butane (assuming a multilayer desorption peak at 108 K) [27], [30] and HCOOH with TDS peaks at 200 K (multilayer peaks according to [20]) and 575 K (CO_2 on HOOH [20]). A linear correction of the readings of the thermocouple was required, with a discrepancy increasing with temperature, which is in agreement with a calibration procedure used before on metal oxide samples [20]. The cleanliness and crystallographic order of the sample have been checked by AES and LEED (see [25]).

3. Presentation of the results

Figure 1 depicts typical examples of adsorption probability measurements. [31] of CO_2 on Cu/ZnO(0001) at small Cu coverage (0.05 ML) (thick solid line), as compared with reference data (from [25]) for the clean ZnO(0001) support (thin solid line). The upper panel shows the raw data, and the lower one the integrated curves. The adsorption temperature is well below CO_2 thermal desorption [25]. Therefore, the coverage is normalized to 1 ML, indicating saturation of the surfaces at the given measuring conditions. Due to the synergistic effects of the deposits and the support (see below), that normalization cannot, however, lead to determining an absolute surface particle density. In the case of CO_2–Cu/ZnO(0001), the uptake (figure 1a) and $S(\Theta)$ (figure 1b) curve, respectively, consist clearly of two regimes (indicated by the dashed lines). The transient starts with a flat part ($S\sim$ const.) which is followed by a linear decrease in S with increasing coverage ($S = 1 - \Theta$ for $\Theta > 0.8$ ML) (figure 1b). This curve shape contrasts the one seen for the clean ZnO(0001) surface, which is characterized by an overall increase in S with Θ, referred to as adsorbate-assisted adsorption (see the solid lines in figure 1 and [27] for details about CO_2–ZnO(0001)). For both systems, S decreases to zero in approaching saturation of the model catalyst with CO_2, as is common for many similar systems. The temperature and impact energy-dependence of $S(\Theta)$ curves follows essentially the same trend, i.e., two regimes are detectable for CO_2–Cu/ZnO(0001). A full account of the measurements will be presented elsewhere. Note, however, that the area above the $S(\Theta)$ curves (and below the dotted line) is larger by approx. 55% for the clean support as compared with Cu/ZnO(0001). That area corresponds to the amount of adsorbed particles. Thus, the saturation coverage of CO_2 on ZnO(0001) is significantly larger than for Cu/ZnO(0001) since the CO_2 flux has been kept constant while measuring both transients.

Figure 2 summarizes the results of the TDS measurements. The spheres depict CO_2-TDS for Cu/ZnO(0001) parametric in Cu pre-exposure and consist of a narrow peak at 103 K (α_3 peak) and a broad structure in the temperature range of 110–170 K (α_4 peak). The thin, solid line is given as a reference and had been obtained for CO_2–ZnO(0001). The α_1 and α_2 peaks can be assigned to CO_2 desorption from pristine and intrinsic defect sites, respectively (see [25] and Section 1). Finally, the inset depicts the TDS results of coadsorption experiments with n-butane. The Cu/ZnO(0001) system has been saturated first with CO_2. Afterwards *n*-butane has been dosed and the adsorbed amount of it subsequently has been determined by *n*-butane TDS. The result of that coadsorption experiment (open spheres) is depicted in comparison with *n*-butane TDS for the clean (thin, solid line) surface; for details see figure 2b in ref. [25] AES measurements obtained after TDS and King and Wells measurements indicated a negligible amount of carbon on the surface.

4. Discussion

4.1. (a) The adsorption probability measurements (adsorption dynamics)

The bimodal shape of the $S(\Theta)$ curves, as obtained on the CO_2/Cu–ZnO(0001) surface, differ clearly from the one measured for the Cu-free support, a result which indicates already a metal support interaction. Note that,

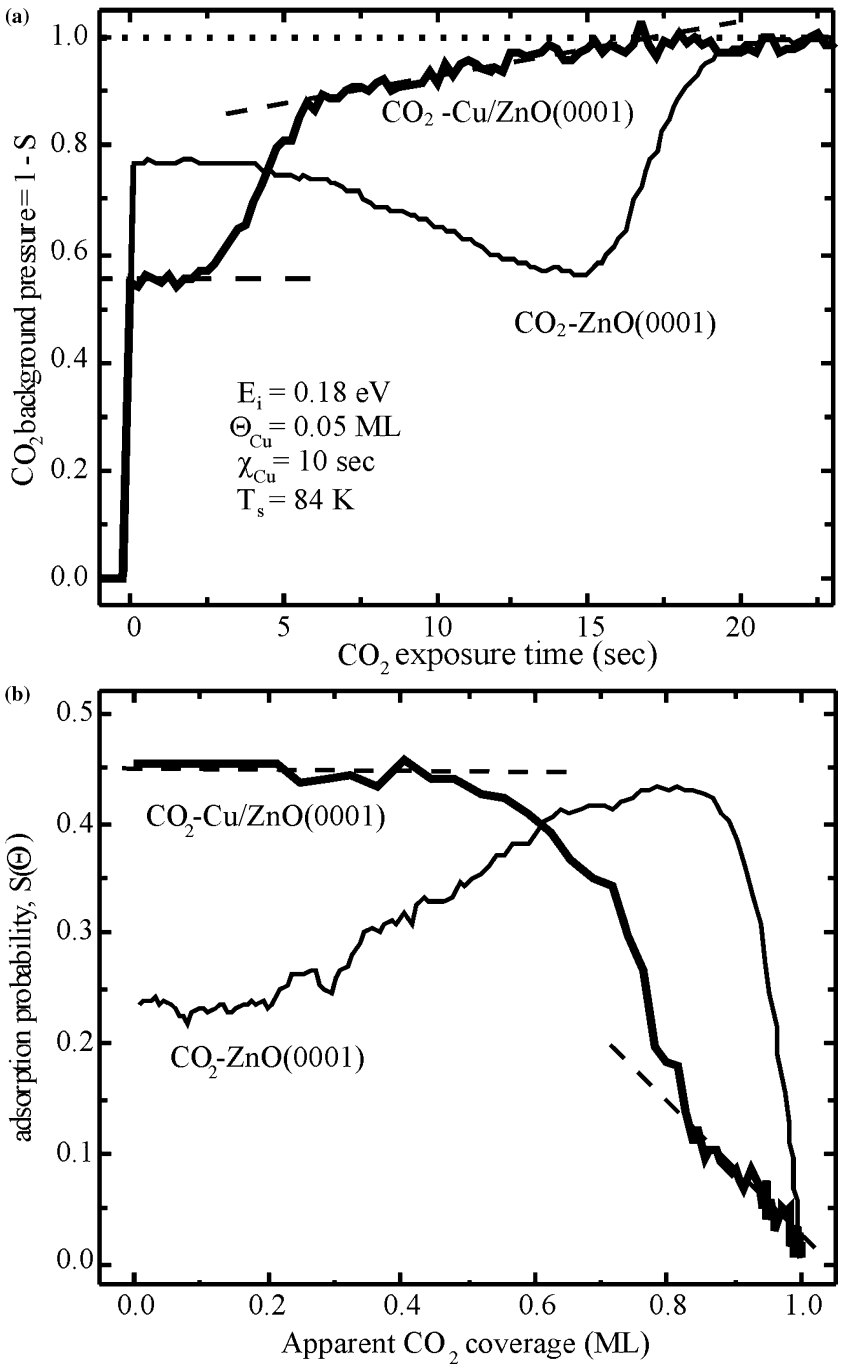

Figure 1. Adsorption probability, *S*, measurements. (a) Raw data, i.e., *S* vs. exposure time for CO_2–Cu/ZnO(0001) (thick solid line) and for ZnO(0001) (thin solid line). (b) Integrated curves, i.e., *S* vs. coverage. The thick line denotes $S(\Theta)$ of CO_2 for Cu/ZnO(0001) and the thin line for ZnO(0001). Additionally indicated are the different adsorption regimes (dashed lines) for CO_2–Cu/Zn(0001). The area above the curves and below the dotted line correspond to the amount of adsorbed CO_2 molecules. (measuring parameters as indicated).

in the case of ZnO(0001), a so-called adsorbate-assisted adsorption (S increases with Θ) has been observed (see thin line in figure 1), which is the result of a strong extrinsic precursor effect (see [27] for details). Therefore, in the case of CO_2/Cu–ZnO(0001), and at a quick glance, the most simple explanation [32] for the bimodal shape (see the thick, solid line in figure 1), might be assuming a dominance of the adsorption dynamics by adsorption events on the zinc oxide support, leading to precursor-mediated adsorption. The Cu deposits might simply act as defects, leading to a turnover from adsorbate-assisted (seen for ZnO(0001)) to Kisliuk-like ($S \sim$ const.) adsorption dynamics (seen for CO_2/Cu–ZnO(0001) up to 0.8 ML)—cf., the Monte Carlo Simulations in ref. [33]. We might then argue that after saturating the support, the Cu particles start to fill up,

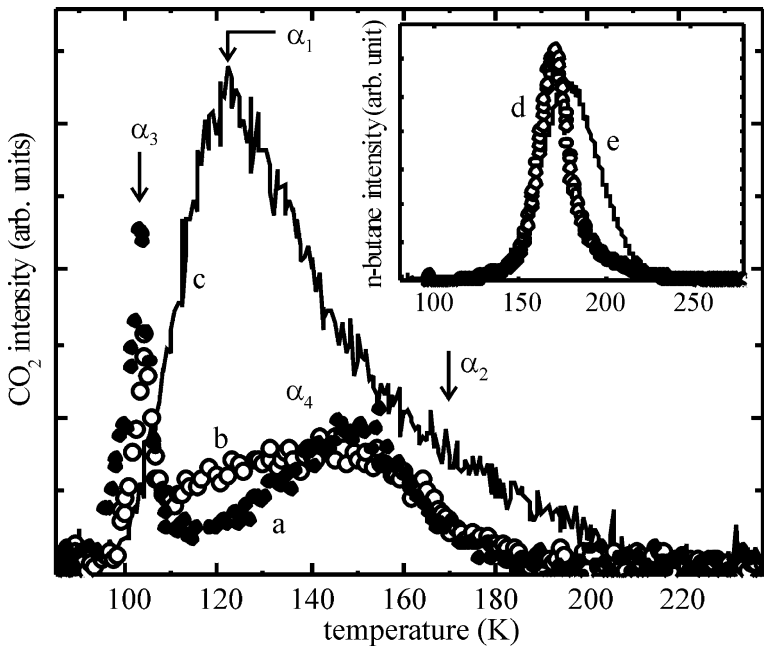

Figure 2. Thermal Desorption Spectroscopy (TDS) curves. (a) CO_2–Cu/ZnO(0001) for small (0.05 ML) Cu coverage. (b) CO_2–Cu/ZnO(0001) for large (1.29 ML) Cu coverage. (c) CO_2 on clean ZnO(0001). (d) *n*-butane TDS obtained for the CO_2 saturated Cu/ZnO(0001) surface (0.05 ML Cu). (e) *n*-butane TDS obtained for the clean ZnO(0001) surface. (Heating rate 1.6 K/sec, 5 L *n*-butane).

leading to a linear decrease in S with Θ above 0.8 ML). That assumption would be consistent with the direct adsorption mechanism ($S \sim 1 - \Theta$) observed for CO adsorption on the nano-sized Cu particles [24]. Additionally, the binding strength of CO_2 on copper single crystals is smaller (25 kJ/mol, see [26]) than on the support (34.4 kJ/mol [25]). Thus, an initial adsorption on the support might be favored kinetically. However, the TDS results (see figure 2) contradict that simple model.

4.2. (b) The TDS measurements (adsorption kinetics)

In comparison with kinetic data on Cu single crystals and the clean ZnO(0001) support, the low temperature TDS peak (at 102 K) can be assigned to desorption from the Cu deposits [26]. Note that the area of the α_3 peak increases only by ~35% within 0.05–1.29 ML of Cu. This result is in agreement with STM data (see Section 1) which indicate that the height of the Cu clusters increase with Cu exposure rather than their lateral dimension (above the critical coverage of ~0.2 ML Cu).

The broad structure (α_4 peak at 110–170 K) is associated with CO_2 adsorption on the support (see [25] for details) and/or along the perimeter of the Cu particles. For the clean ZnO(0001) surface, the separation in two TDS peaks was more distinct, with a low temperature structure at ~120 K (assigned to adsorption on pristine sites) and a high temperature structure at ~150 K (assigned to intrinsic defect sites). The large widths of the α_4 TDS peak indicates, however, already adsorption/desorption of CO_2 from a number of different adsorption sites. Importantly, the area of the α_4 TDS peak is correlated with the Cu exposure. Note that, the temperature of the α_4 TDS peak is larger than the one of the α_1 structure, i.e., Cu appears to stabilize CO_2 as the intrinsic defects did [25]. More important, however, is a comparison of the TDS peak areas obtained after saturating Cu/ZnO(0001) and ZnO(0001) with CO_2.

From the area of the TDS curves, it is evident that the CO_2 saturation coverage on the Cu-free support is larger than the one on CO_2–Cu/ZnO(0001). The area of the α_4 peak is ~65% (approx. independent of Θ_{Cu}) smaller than the total area of the α_1 and α_2 peaks, which is in reasonable agreement with results obtained from the King and Wells measurements (figure 1a). Note that identical CO_2 exposures and heating rates have been applied for all TDS measurements, and the measuring geometry was exactly identical. This leads to the obvious hypothesis that CO_2 adsorbs predominantly on the Cu particles (α_3 TDS peak) and along the rim of the Cu particles (α_4 TDS peak) leaving the Cu-free areas of the support mostly clean.

This model is also consistent with the adsorption dynamics. Following that proposal, and loosely speaking, the Cu particles would act as the "landing site" of the CO_2 molecules but the "hangar" is the rim along the Cu particles. Thus, we have to assume an intrinsic precursor state above the initially clean Cu particles and a subsequent diffusion of the trapped molecules to the perimeter of the Cu particles, where they adsorb. This precursor effect would lead to the Kisliuk-like shape (precursor-assisted adsorption) of the S(Θ) curves, seen up to a CO_2 coverage of 0.8 ML (see figure 1). The rim, now blocked by CO_2 molecules, might act as a high-energy barrier for diffusion of newly (on the Cu clusters)

arriving CO_2 molecules to the ZnO support. In turn, the Cu particles start to be populated by CO_2 leaving, however, the ZnO support mostly CO_2-free. The adsorption of CO_2 on the Cu particles could again be assigned to the linear section of the S(Θ) curves. This scenario would be consistent with the direct adsorption ($S \sim 1 - \Theta$) observed for CO on the Cu deposits (see [24]). Assuming a capture zone [32] for CO_2 around the Cu cluster with a size defined by the effective lifetime (desorption/diffusion) of the adsorbate on the support would also be consistent with the Kisliuk-like section of the $S(\Theta)$ curves.

4.3. (c) Coadsorption TDS results

Arguing by comparing absolute TDS intensities (figure 2) always raises certain doubts. Since we cannot provide spectroscopic data from our laboratory, we applied a simpler approach to check that the Cu-free areas of the ZnO support are indeed CO_2-free after saturating Cu/ZnO(0001) with CO_2. The result of the control experiment is shown as an inset of figure 2. First, the Cu/ZnO(0001) has been saturated with CO_2. Afterwards *n*-butane was exposed on the surface. The *n*-butane TDS curves obtained for the CO_2–Cu/Zn(0001) system indicate that a significant amount of the hydrocarbon still adsorbs on Cu/ZnO(0001), which has already been saturated with CO_2. The adsorption of *n*-butane on the clean ZnO(0001) support was characterized before (see [25]). Accordingly, the TDS curves shown in the inset are typical of *n*-butane adsorption in the monolayer range. (Multilayer would lead to a distinct low temperature TDS peak.) Due to limitations of our sample cooling, we have used a longer chain alkane and not, e.g., CO for the coadsorption experiment. That Cu/ZnO(0001) was initially saturated by CO_2 is evident since we used the molecular beam system for dosing the CO_2, i.e., the King and Wells curves (figure 1) indicate clearly that the surface is indeed saturated.

The amount of Cu needed to modify the chemical behavior of the support is amazingly small (5% ML). However, it is well known that trace amounts of, e.g., alkali metals can significantly alter the work function of metal surfaces (see e.g. [34]) and hence alter their chemistry. Furthermore in catalysis studies, a suppression of CO adsorption on TiO_2-supported metals has been observed before (see e.g. [35]). Additionally, in an early study about the methanol synthesis reaction, J.C. Frost suggested [17] a distinct synergy effect on the metal/oxide junction which is caused by the formation of Schottky barriers. This effect leads to an ionization and creation of oxygen vacancy sites along the Cu cluster.

5. Conclusions

In summary, adsorption probability and different sets of TDS measurements present indications for a metal support interaction in the system Cu-on-ZnO(0001). Accordingly, CO_2 populates predominantly the ZnO support along the rim of the Cu deposits, leaving thereby large parts of the support CO_2-free.

Acknowledgments

This work has been supported by the National Science Foundation (ND-NSF-EPSCoR grant #0132289), and acknowledgment is made as well to the donors of The American Chemical Society Petroleum Research Fund.

References

[1] T.S. Askgaard, J.K. Norskov, C.V. Ovesen and P. Stoltze, J. Catal. 156 (1995) 229.
[2] J.B. Hansen, in *Handbook of Heterogeneous Catalysis*, eds. G. Ertl, H. Knötzinger and J. Weitkamp, (VCH, 2001).
[3] K. Klier, Adv. Catal. 31 (1982) 243.
[4] B.S. Clausen and H. Topsoe, Catal. Today 9 (1991) 189.
[5] J. Yoshihara and C.T. Campbell, J. Catal. 161 (1996) 776.
[6] P.L. Hansen, J.B. Wagner, S. Helveg, J.R. Rostrup-Nielsen, B.S. Clausen and H. Topsoe, Science 295 (2002) 2053.
[7] J.D. Grunwaldt, A.M. Molenbroek, N.Y. Topsoe, H. Topsoe and B.S. Clausen, J. Catal. 194 (2000) 452.
[8] K.D. Jung, O.S. Joo and S.H. Han, Catal. Lett. 68 (2000) 49.
[9] H. Nakatsuji and Z.M. Hu, Intern. J. Quantum Chem. 77 (2000) 341.
[10] I. Nakamura, H. Nakano, T. Fujitani, T. Uchijima and J. Nakamura, Surf. Sci. 402–404 (1998) 92.
[11] K.C. Waugh, Catal Lett. 58 (1999) 163.
[12] S.A. French, Angew. Chem. 113 (2001) 4569.
[13] D.W. Goodman, J. Catal. Lett. 99 (2005) 1.
[14] R. Meyer, M. Baumer, S.K. Shaikhutdinov and H.J. Freund, Surf. Sci. 546 (2003) L813.
[15] Q. Fu, T. Wagner, S. Olliges and H.D. Carstanjen, J. Phys. Chem. 109 (2005) 944.
[16] G.A. Somorjai.
[17] J.C. Frost, Nature 334 (1988) 577.
[18] S.V. Didziulis, K.D. Butcher, S.L. Cohen and E.I. Solomon, J. Am. Chem. Soc. 111 (1989) 7110.
[19] G. Thornton, S. Crook and Z. Chang, Surf. Sci. 415 (1998) 122.
[20] J. Yoshihara and C.T. Campbell, Surf. Sci. 407 (1998) 256.
[21] B. Meyer and D. Marx, Phys. Rev. B 69 (2004) 235420.
[22] G. Kresse, O. Dulub and U. Diebold, Phys. Rev. B 68 (2003) 245409.
[23] J. Yoshihara, J.M. Campbell and C.T. Campbell, Surf. Sci. 406 (1998) 235.
[24] J. Wang and E. Johnson, U. Burghaus, Chem. Phys. Lett. (in press).
[25] J. Wang, B. Hokkanen and U. Burghaus, Surf. Sci. 577 (2005) 158.
[26] K.H. Ernst, D. Schlatterbeck and K. Christmann, Phys. Chem. Chem. Phys. 1 (1999) 4105.
[27] J. Wang and U. Burghaus, J. Chem. Phys. 122 (2005) 044705-11.
[28] D.W. Goodmann, J. Chem. Phys. 100 (1996) 13090.
[29] U. Burghaus, J. Ding and W.H. Weinberg, Surf. Sci. 396 (1998) 273.
[30] C. Xu, B.E. Koel and M.T. Paffett, Langmuir 10 (1994) 166.
[31] D.A. King and M.G. Wells, Surf. Sci. 29 (1972) 454.
[32] F. Rumpf, H. Poppa and M. Boudard, Langmuir 4 (1988) 722.
[33] J. Stephan and U. Burghaus, Surf. Sci. 507–510 (2002) 736.
[34] H.B. Nielsen, U. Burghaus, G. Broström and E. Matthias, Surf. Sci. 234 (1990) L271.
[35] S.J. Tauster, S.C. Fung, R.T.K. Baker and J.A. Horsley, Science 211 (1981) 1121.